BRL-TR-3251

AD-A239 666

(2)

TECHNICAL REPORT BRL-TR-3251

BRL

STRAIN RATE INSENSITIVITY OF DAMAGE-INDUCED SURFACE AREA IN M30 AND JA2 GUN PROPELLANTS

GEORGE A. GAZONAS
ARPAD JUHASZ
JAMES C. FORD

AUGUST 1991

U.S. ARMY LABORATORY COMMAND

BALLISTIC RESEARCH LABORATORY
ABERDEEN PROVING GROUND, MARYLAND

NOTICES

UNCLASSIFIED

REPORT DOCUMENT PAGE	Form Approved OMB No. 0704-0188

Public reporting burden for this collection of information is estimated to average 1 hour per response, including the time for reviewing instructions, searching existing data sources, gathering and maintaining the data needed, and completing and reviewing the collection of information. Send comments regarding this burden estimate or any other aspect of this collection of information, including suggestions for reducing this burden, to Washington Headquarters Services, Directorate for Information Operations and Reports, 1215 Jefferson Davis Highway, Suite 1204, Arlington, VA 22202-4302, and to the Office of Management and Budget, Paperwork Reduction Project(0704-0188), Washington, DC 20503.

1. AGENCY USE ONLY (Leave blank)	2. REPORT DATE	3. REPORT TYPE AND DATES COVERED
	August 1991	Final, Feb 91 - Apr 91

4. TITLE AND SUBTITLE
Strain Rate Insensitivity of Damage-Induced Surface Area in M30 and JA2 Gun Propellants

5. FUNDING NUMBERS
PR: 1L161102AH43

6. AUTHOR(S)
George A. Gazonas, Arpad Juhasz, and James C. Ford

7. PERFORMING ORGANIZATION NAME(S) AND ADDRESS(ES)
USA Ballistic Research Laboratory
ATTN: SLCBR-IB-P
Aberdeen Proving Ground, MD 21005-5066

8. PERFORMING ORGANIZATION REPORT NUMBER

9. SPONSORING/MONITORING AGENCY NAMES(S) AND ADDRESS(ES)
USA Ballistic Research Laboratory
ATTN: SLCBR-DD-T
Aberdeen Proving Ground, MD 21005-5066

10. SPONSORING/MONITORING AGENCY REPORT NUMBER
BRL-TR-3251

11. SUPPLEMENTARY NOTES

12a. DISTRIBUTION/AVAILABILITY STATEMENT
Approved for public release; distribution is unlimited.

12b. DISTRIBUTION CODE

13. ABSTRACT (Maximum 200 words)

Uniaxial compression tests are performed at constant strain rate on single-grain, seven-perforated specimens of M30 and JA2 gun propellant using the US Army's high rate, servohydraulic test apparatus in order to investigate the effects of strain rate, temperature, and percent axial strain on the combustion characteristics (apparent burn rate and pressurization rate) of the propellants. At room temperature M30 primarily deforms by macroscopic fracture and JA2 deforms by macroscopic flow. The total number of tests (sixteen) is minimized by designing the experimental program according to a 2^4 statistical design strategy. The single grains of deformed propellant are then burned in a newly designed 7.8-cc mini closed-bomb and plots of pressure, pressurization rate and surface area ratio versus time, and apparent burn rate versus pressure are compared with baseline results for the undeformed propellant specimens. The apparent burn rates of damaged M30 propellant vary considerably and the degree of damage-induced surface area approaches six times that of the undeformed baseline M30 specimens. The apparent burn rates of JA2 are relatively unaffected by the induced deformation. Results of the statistical test design indicate that the apparent burn rate of JA2 at 20 MPa is primarily dependent on the deformation temperature, yet the apparent burn rate of M30 at 20 MPa is dependent primarily on percent axial specimen strain. The apparent burn rates for these propellants are relatively insensitive to the deformation strain rate over the range 10^{-2} to 100 sec^{-1}.

14. SUBJECT TERMS
Burn Rate Analysis, Mini Closed-Bomb, Propellants, JA2, M30 Statistical Design Screening Design, Burning Rate

15. NUMBER OF PAGES
38

16. PRICE CODE

17. SECURITY CLASSIFICATION OF REPORT	18. SECURITY CLASSIFICATION OF THIS PAGE	19. SECURITY CLASSIFICATION OF ABSTRACT	20. LIMITATION OF ABSTRACT
UNCLASSIFIED	UNCLASSIFIED	UNCLASSIFIED	UL

NSN 7540-01-280-5500

Standard Form 298 (Rev 2-89)
Prescribed by ANSI Std 239-18
298-102

UNCLASSIFIED

INTENTIONALLY LEFT BLANK.

TABLE OF CONTENTS

INTENTIONALLY LEFT BLANK.

LIST OF FIGURES

INTENTIONALLY LEFT BLANK.

LIST OF TABLES

INTENTIONALLY LEFT BLANK.

ACKNOWLEDGEMENTS

We wish to thank Dan Bullock for his help in fielding the Closed Bomb (CB) tests, Bill Aungst and Steve Fortier for conducting the CB experiments, and Sharon Richardson for performing the initial CB data reduction and analysis.

INTENTIONALLY LEFT BLANK.

1. INTRODUCTION

The ignition of gun propellant occurs when hot primer gases come into contact with the exposed surfaces of the propellant. Thermal energy is conducted into the propellant and combustion occurs at points where the local ignition temperature is reached. As the propellant begins to burn, combustion products are given off which raise the ambient chamber pressure. The regression rate or burn rate of the propellant is observed to be a strong function of pressure.

One might argue that propellant burn rate should be viewed as an intrinsic property of a particular propellant formulation (i.e. chemical composition). However, propellants with identical chemical composition could have different "intrinsic" burn rates if they possess different microstructural fabrics. This is particularly true if the propellants are manufactured by different processes. For example, one might measure different burn rates in two chemically identical lots of M30 if one lot has a distinctly higher porosity than the other lot. In reference to pressed HMX explosives, Fifer and Cole[1] distinguish between burn rate as a "fundamental property of explosive materials" and regression rate which describes deflagration that is additionally dependent upon the physical properties of the charge such as: porosity, permeability, and grain size. In this research, the term apparent burn rate is considered synonymous with Fifer and Cole's regression rate. If the porosity present in a particular propellant is interconnected and forms a surface area network along which hot combustion gases can infiltrate then regression rates should be greater than for chemically identical, less permeable propellant. Such materials would have high gas or "flame" permeabilities. Propellant permeability would also increase through fracture damage induced by a rapidly fluctuating multiaxial stress field present in the gun tube during firing. An increase in a propellant's fracture permeability due to deformation enhances the propellant's susceptibility or vulnerability to convective burning "hot gas infiltration" mechanisms. Many of these concepts are illustrated in Figure 1 which shows the intrinsic burn rate, R_i, of a propellant blob with intrinsic permeability, K_i. Extrusion manufacturing processes can induce a variety of flaw sizes and distributions in the propellant, and if the flaws are interconnected the propellant will possess a permeability, K_{cd1} (subscript cd1 stands for crack density 1). If hot convective gases infiltrate through the crack permeability during combustion, then the apparent burn rate, R_{cd1}, will be greater than the intrinsic burn rate of the "Ideal Propellant" (Figure 1).

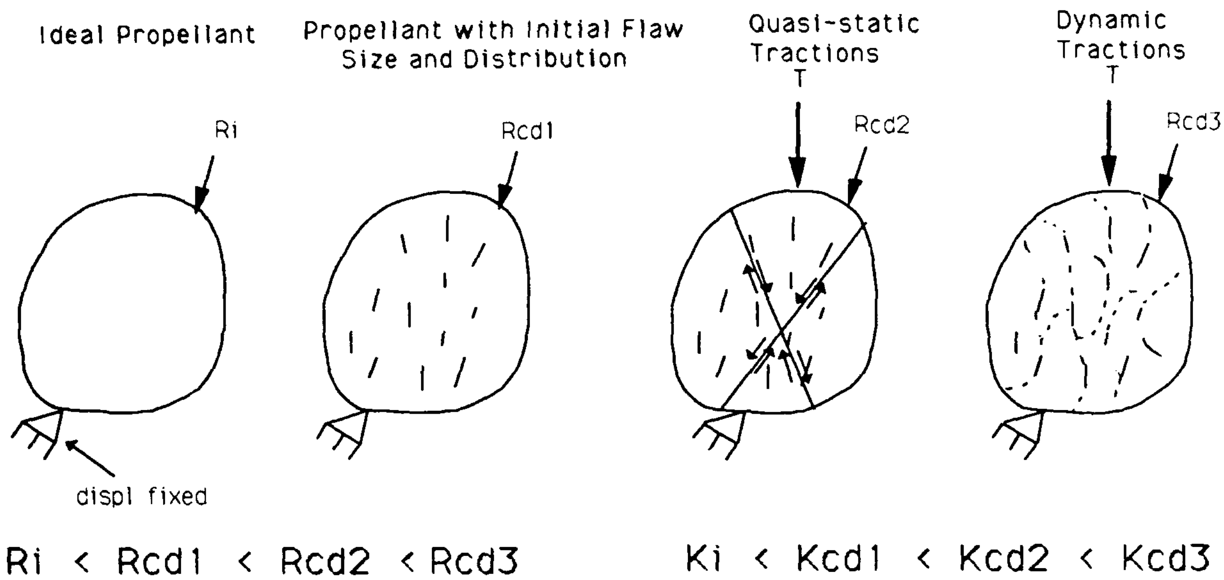

Figure 1. Intrinsic and Apparent Burning Rate in Solid Propellant with Augmentation of Burn Rate as a Function of Loading Rate.

Experimental results of mini closed-bomb tests on damaged propellant grains indicate that fracture surface area dramatically increases in damaged propellant leading to anomalously high pressurization rates during combustion[2,3]. Many materials do not deform by fracture mechanisms so surface area changes in the propellant due to fracturing must be partitioned from strain-induced dimensional surface area changes in the propellant. At present, interior ballistic models (e.g., NOVA, XNOVAKTC)[4] calculate the hydrostatic component of the stress tensor (pressure) as well as the axial component of intergranular solid grain stress as a function of position and time in the gun tube. The magnitude of intergranular stress is used in a rudimentary model of grain fracture. The ultimate aim of the present research is to establish a unique relationship, if one exists, between the conditions necessary for propellant failure (i.e., a failure criterion which is often couched in terms of stress or strain invariants, or a critical energy release rate) and time-dependent surface area evolution in the propellant.

The present research examines the effects of strain rate, temperature, and percent axial strain on the combustion characteristics of single grain specimens of M30 and JA2 gun propellant. The choice of these variables is motivated by the observation that the mechanical response of these materials is rate-sensitive

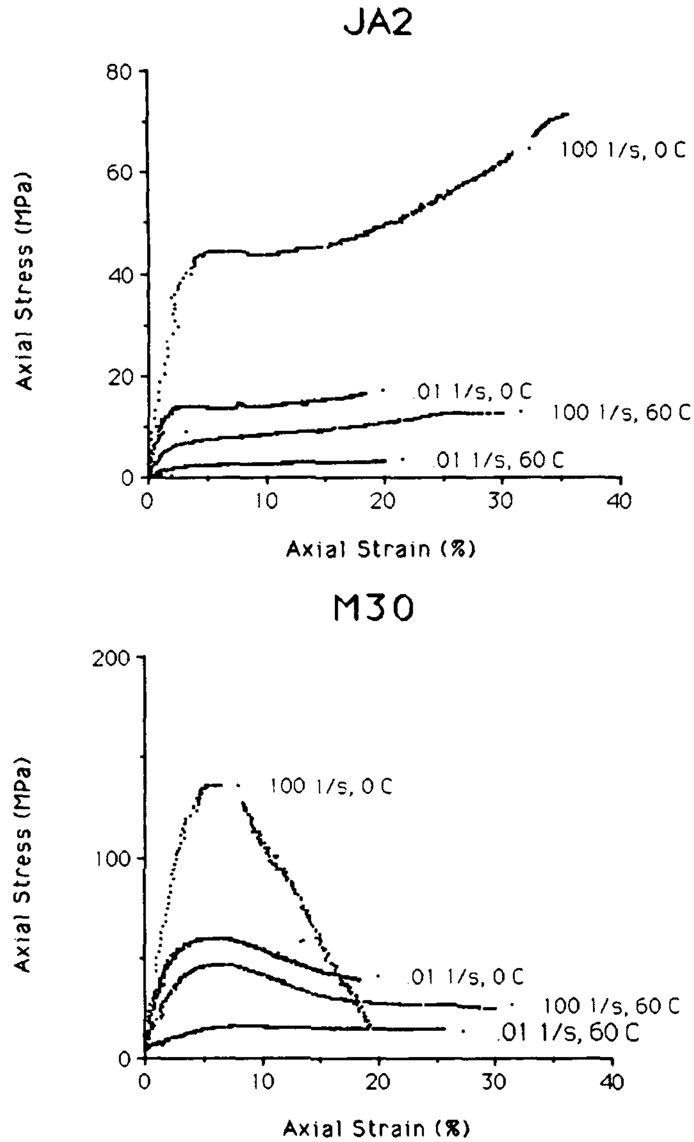

Figure 2. Comparative Mechanical Response of JA2 and M30 Showing Ductile Workhardening JA2 Behavior and Ductile Worksoftening M30 Behavior.

and temperature-sensitive[2,3,5,6] (Figure 2). In addition, observations indicate that the fragmentation size in a wide variety of materials is loading rate dependent[7,8]. Fragment size is generally smaller and more highly comminuted in materials subjected to dynamic deformation because stress levels are relatively high throughout the material and cracks initiate and propagate simultaneously. In contrast, fragment size is larger in materials subjected to quasi-static deformation and only those critically oriented cracks will begin to propagate. Eventually the propagation paths will intersect and large throughgoing fractures will develop along which shear displacements occur (Figure 1). Furthermore, we expect the degree of

fracture surface area to increase as the axial specimen strain increases. The M30 and JA2 propellants are chosen since they represent endpoints in material behavior insofar as M30 reaches a maximum stress and deforms by worksoftening mechanisms and JA2 deforms by workhardening mechanisms throughout its deformation history[5] (Figure 2). Briefly, the experimental program will proceed by deforming propellant grains in uniaxial compression, burning the same single propellant grains in a mini closed-bomb, and then comparing the combustion characteristics of the damaged propellant relative to the undamaged propellant in order to determine the relative or hierarchial importance of the test conditions in controlling combustion.

2. EXPERIMENTAL METHOD

2.1 Specimen Preparation Right circular cylinders of M30 (lot # 67878) and German JA2 (lot # NC1013180) propellant are cut from seven-perforation granular stock using an Isomet double-bladed diamond saw. A double-bladed saw is used to cut specimen ends parallel to each other and to help maintain coaxial deformation with the cylinder axis. Nominal dimensions, masses and chemical compositions of the M30 and JA2 specimens appear in Table 1 below.

Table 1. Nominal Percent Chemical Compositions and Dimensions of JA2 and M30 Propellants.

Propellant	JA2	M30
Component	%	%
Nitrocellulose	59.0	28.0
Nitroglycerin	15.0	22.0
Nitroguanidine	0.0	48.0
Ethyl Centralite	0.0	2.0
Diethylene-Glycol Dinitrate	25.0	0.0
Akardit II	1.0	0.0
NC Nitration Level	13.0	12.6
Length (mm)	10.70	10.80
Diameter (mm)	8.80	7.15
Perforation Diameter (mm)	0.508	0.711
Mass (gm)	0.99	0.65

The inert lubricant, molybdenum disulfide, MoS_2, is applied sparingly to the specimen ends since it is found that the variability in mechanical response is reduced in compression testing of these materials when the specimen ends are lubricated[6].

2.2 Servohydraulic Test Apparatus The high rate 810 MTS material test system (Figure 3) consists of a conventional two-pole press with a servohydraulically actuated ram that operates from quasi-static velocities to a maximum velocity of about 12 m/sec; the maximum velocity imparts a maximum strain rate of 1200 sec^{-1} on a 10 mm long specimen. A Thermotron conditioning oven/refrigerator surrounds both upper and lower pistons and permits temperature testing from -85 to 90 degrees Celsius. Specimens are uniformly heated and thermally conditioned at the testing temperature for at least 30 minutes before testing. Uniaxial compression tests are performed at constant strain rate by computer control of the piston velocity via feedback from an externally mounted displacement transducer (LVDT). Force measurements are made with a 60 kN quartz piezoelectric force gage that is mounted on the upper moving piston. Apparatus stiffness is on the order of 97 kN/mm. A more complete description of the servohydraulic apparatus can be found in Gazonas[5].

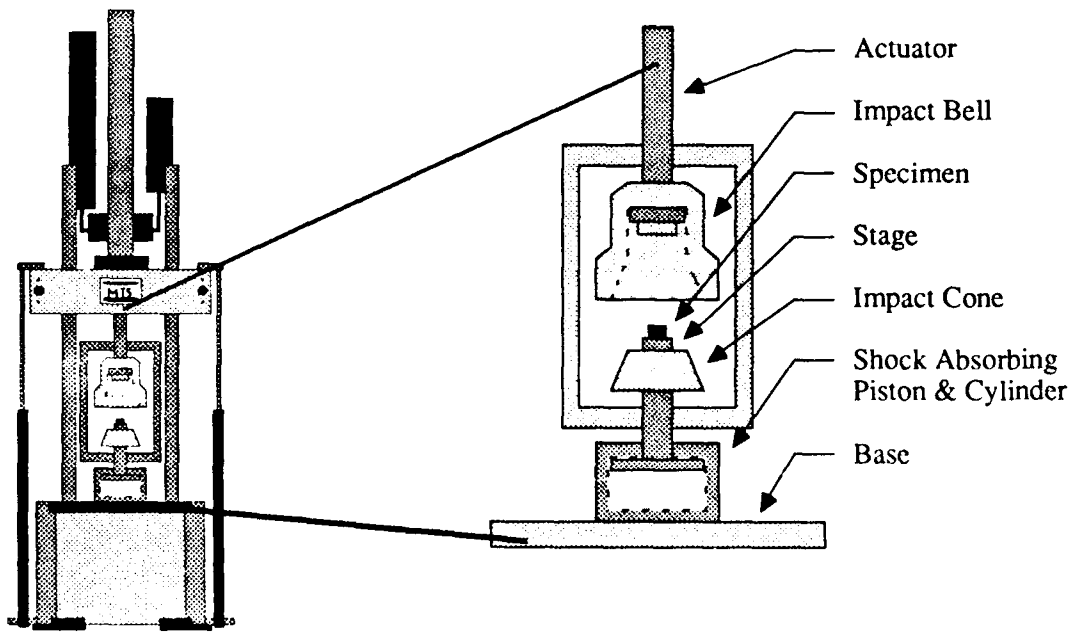

Figure 3. Servohydraulic Apparatus with Upper Bell and Impact Cone Piston Assembly.

The raw force and displacement data are acquired, stored and analyzed using an IQ-300 multichannel processing digital oscilloscope. The raw force and displacement data are reduced to engineering stress versus strain by normalizing to initial specimen area and length, respectively. After the data are analyzed, a variety of mechanical property parameters and pertinent test information are transferred to a Compaq 286 personal computer via RS232 communications port and imported to a DBASE III Plus database library. A total of 31 fields are stored and include propellant I.D., lot, date, compressive modulus, stress and strain at yield, energy absorbed at fixed strain levels from .025 to .25, specimen dimensions, test temperature, strain rate, as well as a character array for a physical description of the deformed propellant.

2.3 Mini Closed-Bomb A new 7.8-cc mini closed-bomb, designed at BRL and manufactured at Harwood Engineering Company, is used to burn the deformed propellant specimens (Figure 4). The ignition primer for these tests consists of 0.2 gms of black powder which is ignited via electric match. Chamber pressure is monitored as a function of time at a sampling frequency of .01 megahertz using a 100-kpsi quartz piezoelectric pressure gage that transmits charge-amplified signals to a Nicolet digital oscilloscope. The voltage versus time data are stored on 5.25" floppy diskettes and converted to ASCII

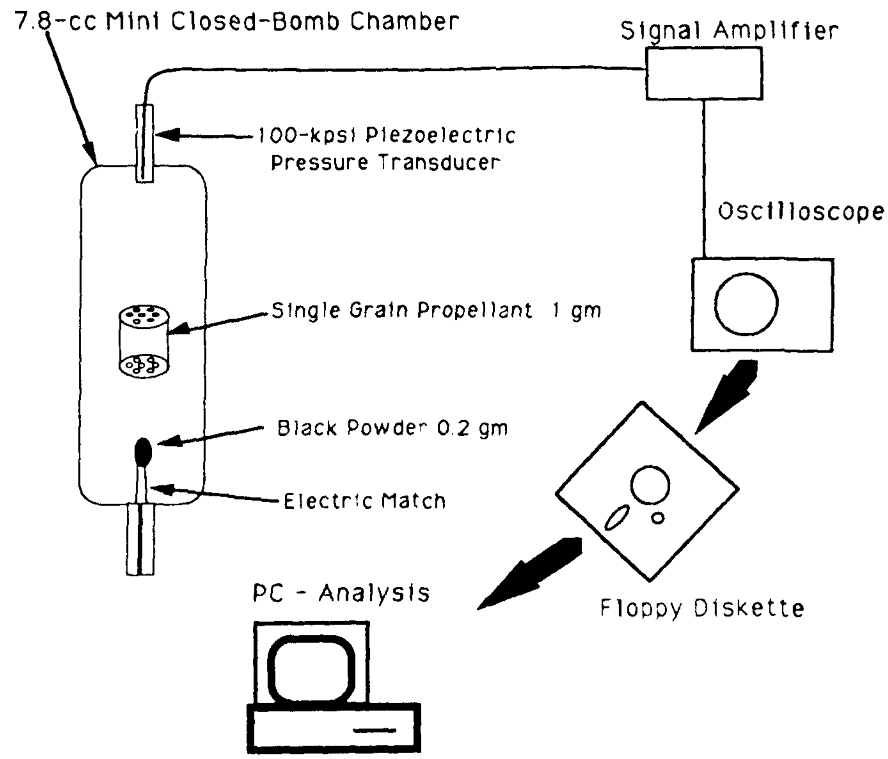

Figure 4. Mini Closed-Bomb Data Reduction and Analysis.

format for burn rate analysis using the BRLCB program[9]. A more complete description of the 7.8-cc mini closed-bomb will appear in a companion report.

The relationship between the mass generation rate, dm/dt, surface area, A, and the burn rate, R, of the propellant is given by:

$$dm/dt = rho * A(t) * R \qquad (1)$$

where,

m = gaseous mass (g)

rho = propellant density (g/cc)

A = time dependent surface area (sq. cm)

R = burn rate (cm/sec)

An empirical relationship for the burn rate, R, is given by:

$$R = a * P^n \qquad (2)$$

where, P, is pressure (MPa), and a and n are empirically determined constants. The mass generation rate on the left-hand side of Equation 1 is a function of the gas pressurization rate, bomb volume, temperature, propellant physical properties and thermochemical constants[9,10]. The time dependent area, A(t), in Equation 1 is an explicit function of the initial propellant geometry and the depth burnt, so that one can explicitly solve for the burn rate, R. Baseline burn rate versus pressure plots (Equation 2) for M30 and JA2 are highly reproducible (Figure 5) and there is good agreement between plots of burn rate versus pressure for the 7.8-cc mini closed-bomb (single grain) and the 200-cc closed-bomb (50-60 grains) (Figure 6). The remarkable agreement between single-grain and multiple-grain burn rate results might be attributed to the relative rapid rate of flamespreading (20 times linear burn rates) observed in linear arrays of LOVA propellant[11].

3. EXPERIMENTAL DESIGN

The "classical" one-factor-at-a-time[12] test program proceeds by testing over the operating range of a particular variable, while the other variables are held constant at a value within their respective ranges. The test program can become time consuming and costly if the effects of a number of variables are to be investigated. Furthermore, if nonlinear interaction effects are present among the variables, one-factor-at-a-time experimentation will not detect them. For example, suppose that a series of tests are

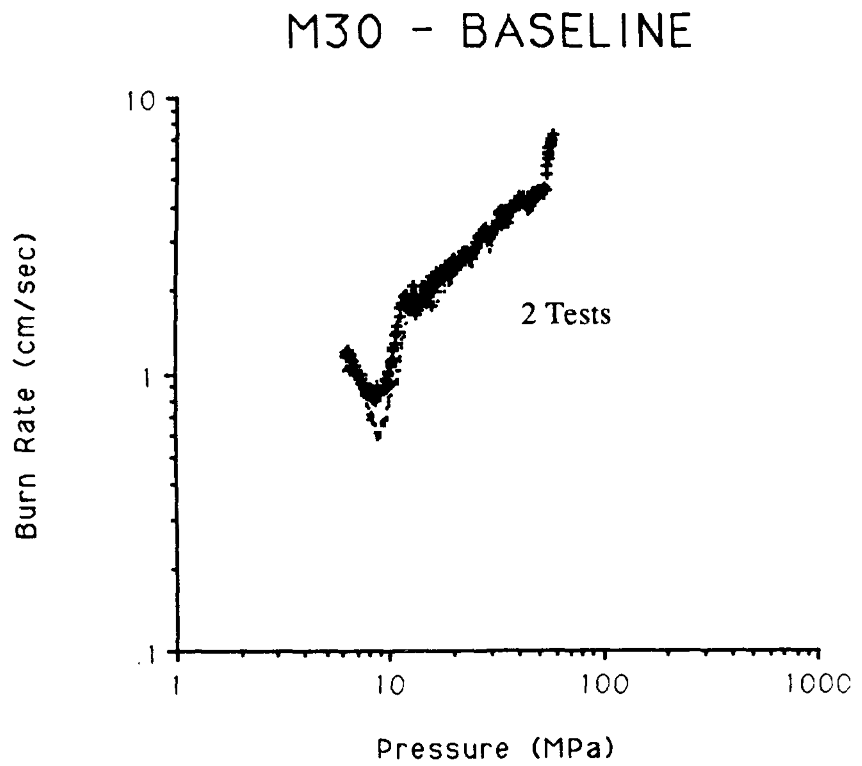

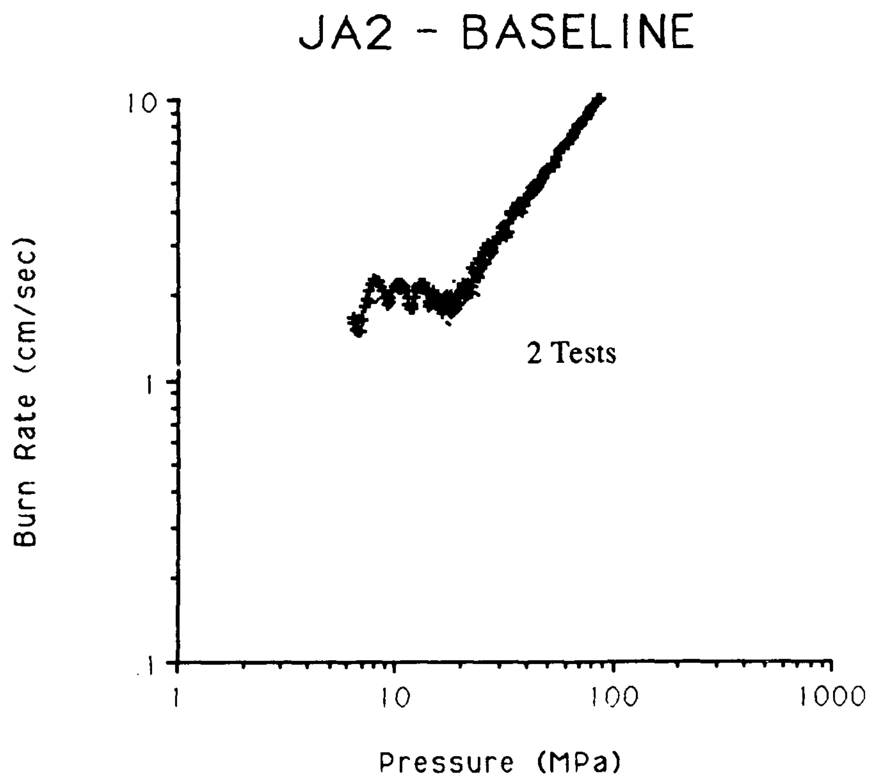

Figure 5. Reproducibility of Burn Rate versus Pressure in Baseline Undamaged M30 and JA2. Coordinate Axes are Log Base 10.

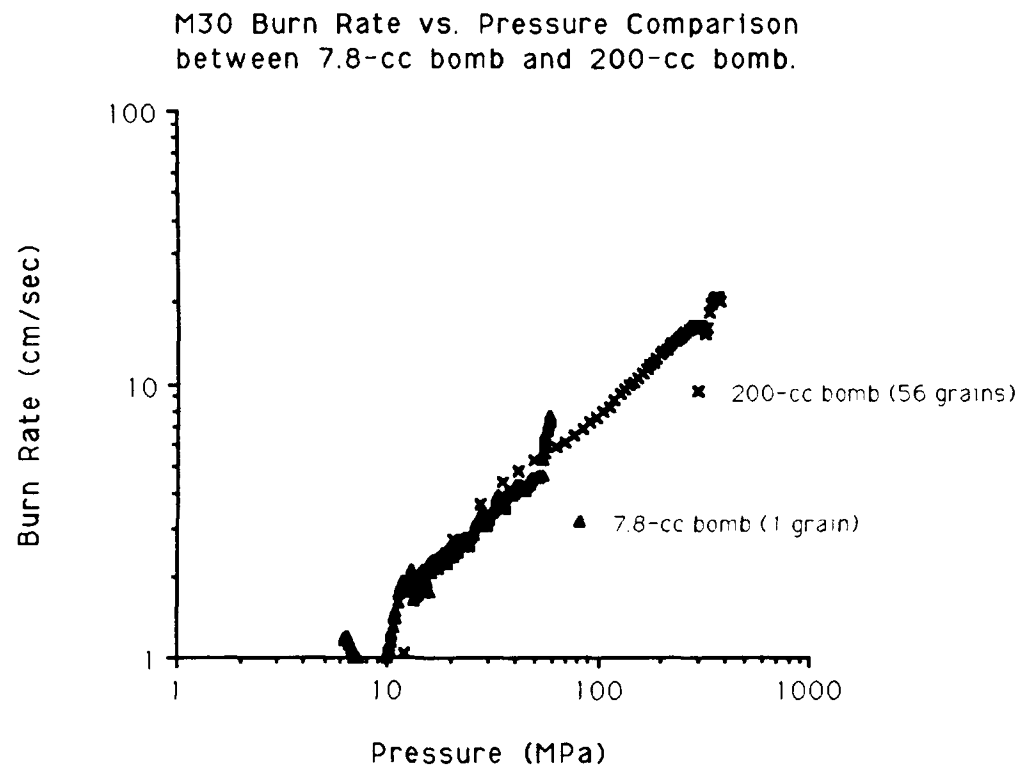

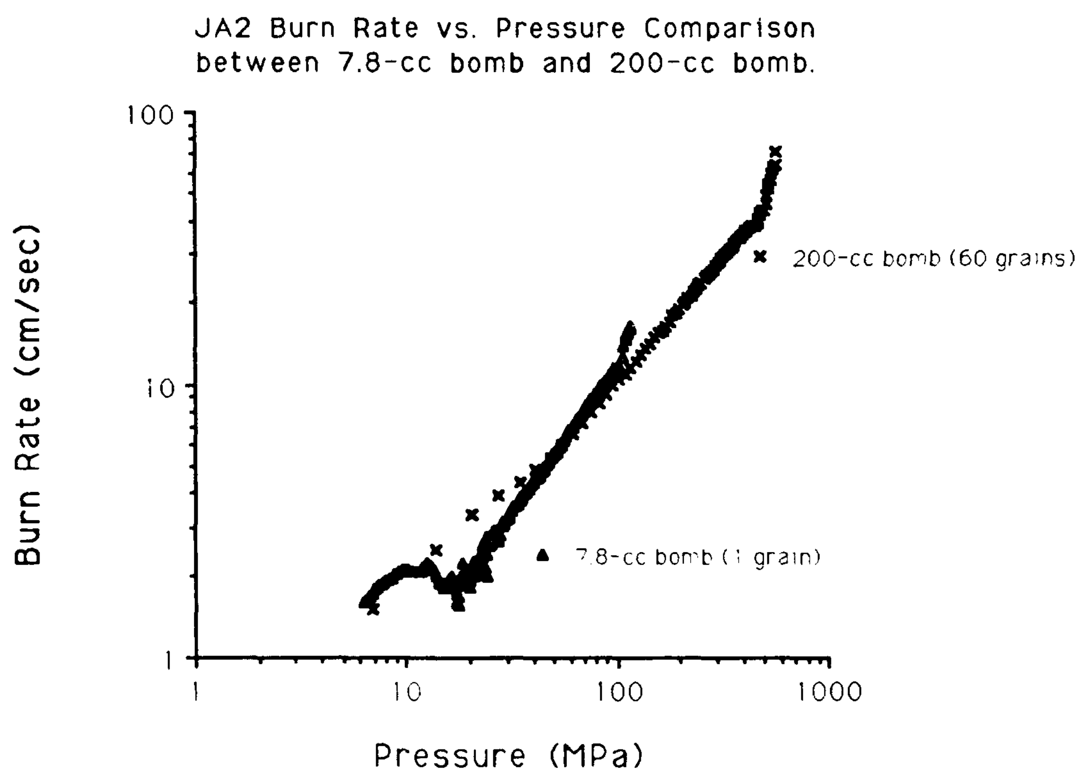

Figure 6. Comparison of Burn Rate versus Pressure between 7.8-cc Mini Closed-Bomb and 200-cc Closed-Bomb for M30 and JA2 Propellants. Coordinate Axes are Log Base 10.

conducted where a response, Y, is measured at various temperatures in order to find the temperature, T_o, at which the response is a maximum (Figure 7a). If the temperature is then held constant at $T=T_o$ and a second series of tests are conducted where the response is measured at various relative humidities (Figure 7b) one could also determine the relative humidity, H_o, at which the maximum response occurs and incorrectly assume that the maximum response is at $T=T_o$, and $H=H_o$ (at x in Figure 7c); the actual interaction response surface could be highly nonlinear and one has a better chance of identifiying the maximum response (within the 50 contour in Figure 7c) with a suitably designed testing or sampling strategy. The simplest sampling strategy involves testing at the factor extremes, "high" and "low", the limits of which are decided upon by the experimenter who is guided by intuition, theory, or limitations of the physical process.

In this research, a 2^4 (factorial) experimental design[12] is used to determine the effects of the continuous variables strain rate, temperature, and percent axial strain, and the discrete variable propellant

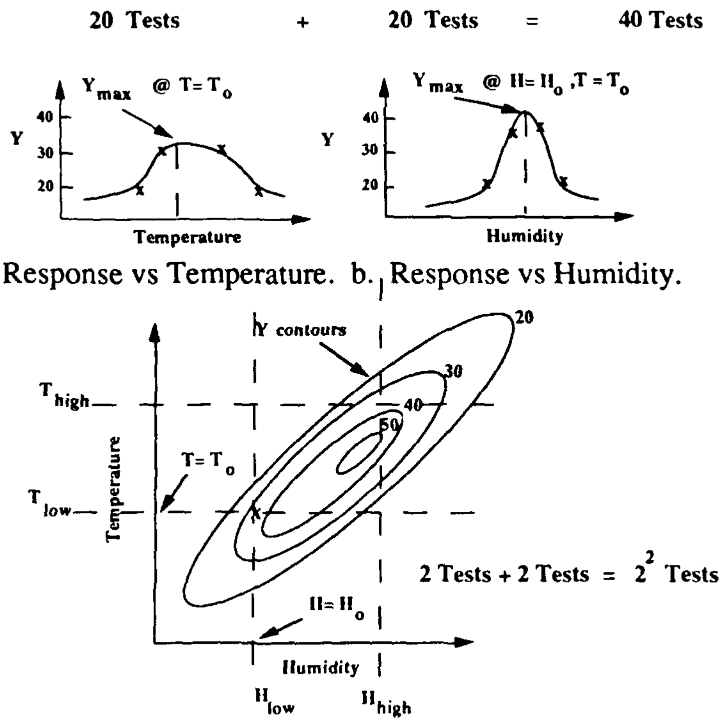

c. Response Interaction Between Temperature and Humidity.

Figure 7. Detection of Nonlinear Interactions using "Classical" and "Statistical" Design Approaches.

Table 2. 2^4 Factorial Experimental Design Randomized Test Sequence.

Test #	Material	Temperature (°C)	Strain Rate (1/s)	% Strain
1	JA2	60	.01	10
2	M30	0	.01	10
3	JA2	0	100	10
4	M30	60	100	10
5	M30	0	100	35
6	JA2	60	100	35
7	JA2	0	.01	35
8	M30	60	.01	35
9	JA2	60	100	10
10	JA2	0	.01	10
11	JA2	60	.01	35
12	M30	0	100	10
13	M30	60	100	35
14	M30	60	.01	10
15	M30	0	.01	35
16	JA2	0	100	35

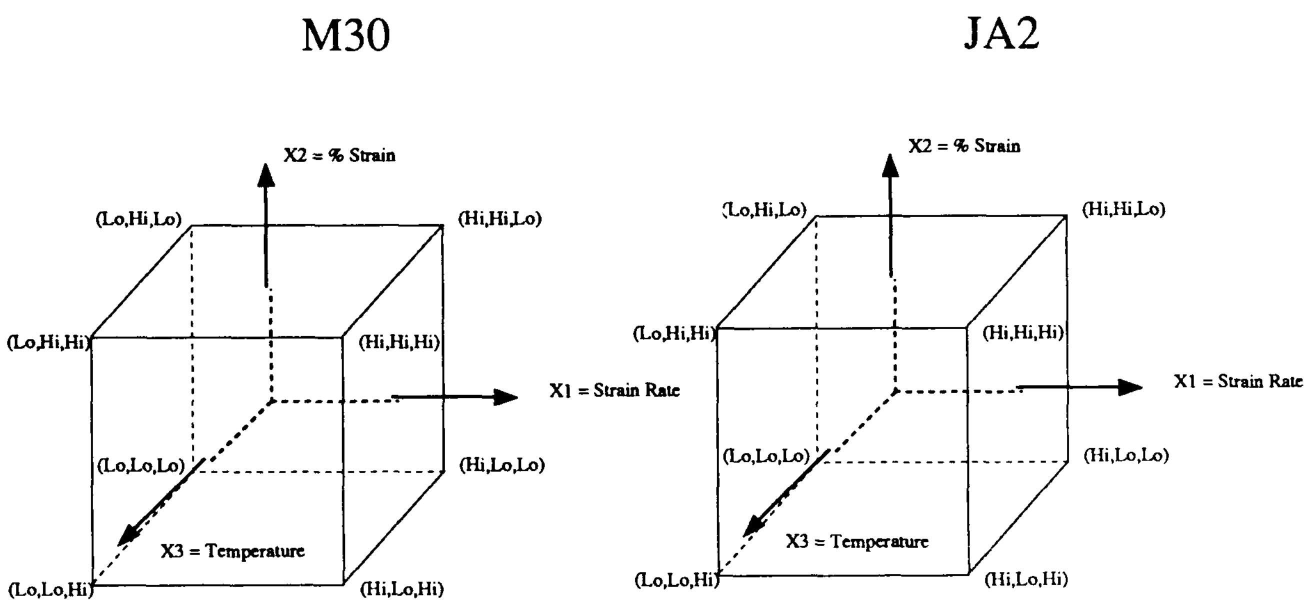

Figure 8. Cube Plots Showing Hi-Lo Experimental Endpoint Combinations for a 2^4 Test Design.

type on apparent burn rate. The design has four independent controllable variables tested at two levels (low and high). The total number of low/high combinations is 2^4 or sixteen experiments. Instrumental carryover error is minimized by conducting the experiments in random order (Table 2).

One can visualize the design endpoints in the 2^4 experimental design using cube plots where each cube vertex represents a particular combination of "low" and "high" test conditions. Two cube plots are needed to represent the sixteen experiments in our 2^4 design; one cube represents all M30 tests and the one cube represents all JA2 tests (Figure 8). A desirable feature of the family of factorial designs is the ability to accommodate both continuous and discrete variables. In addition, the total number of tests can be significantly reduced using a factorial design. Using a "classical" test design, if a response, Y, is measured at four temperatures and relative humidities, then forty tests are required (assuming five replicate tests are conducted at each temperature and relative humidity). In contrast, a 2^2 factorial design requires only four tests at high and low temperatures and relative humidities (Figure 7c). The actual number of tests required at each experimental condition, using the "classical" test approach, is directly proportional to the variance of the measured quantity and inversely proportional to the required tolerance[13]. In a subsequent section it is shown that the combustion response is calculated at each experimental design endpoint using a second degree polynomial equation.

After the experimental design sequence is executed, the damaged propellant grains are burned in the 7.8-cc mini closed-bomb and the combustion characteristics are analyzed using BRLCB[9]. An overview of the experimental results appears in the next section.

4. EXPERIMENTAL RESULTS

4.1 Propellant Mechanical Properties This section outlines the mechanical properties obtained as a result of uniaxial compression testing on M30 and JA2 propellants. The M30 and JA2 gun propellants behave in a macroscopically ductile fashion by sustaining a maximum of 35 percent axial shortening over the temperature range (0 to 60 degrees Celsius) and strain rate range (.01 to 100 sec^{-1}). However, JA2 continually workhardens throughout the deformation history whereas M30 reaches a maximum stress and subsequently worksoftens throughout the deformation history (Figure 2). There are no observable fractures in any of the JA2 specimens (Figure 9), however, M30 specimens 5, 8, 13 and 15, (all shortened 35 percent) initially develop axial cracks which have a tendency to shear and kink with increasing axial

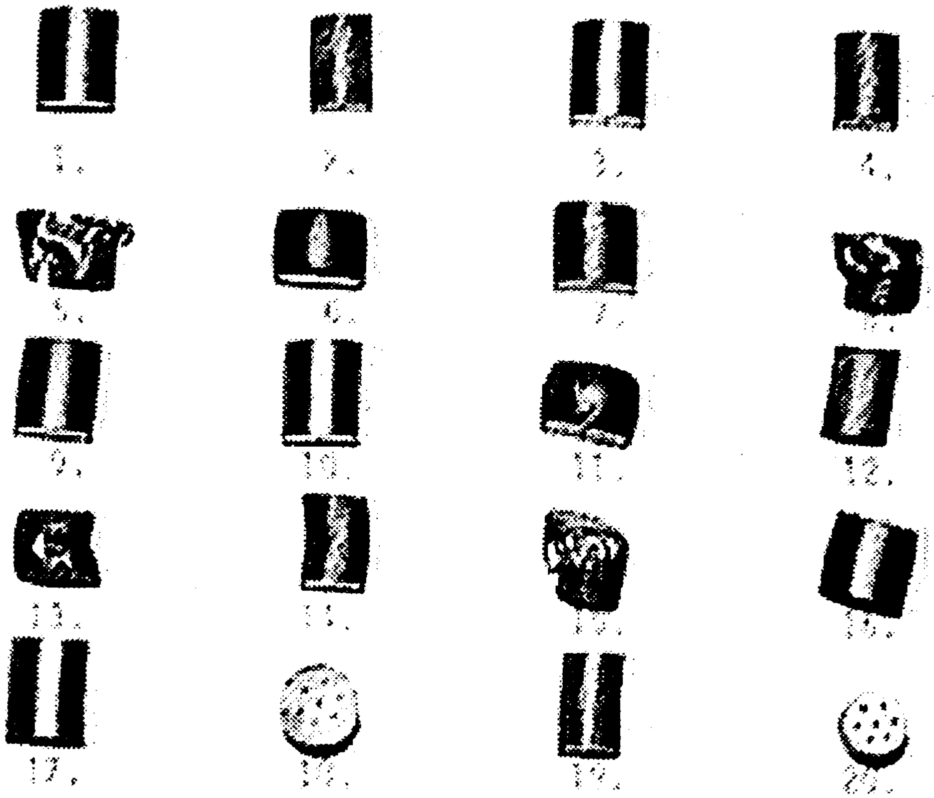

Figure 9. Damaged Propellant Grains According to Conditions in Table 2. Baseline JA2 and M30 are tests 17, 18 and 19, 20 Respectively.

Table 3. Comparative Mechanical Properties for M30 and JA2 Gun Propellant versus Temperature and Strain Rate.

Material	Temp.(°C)	S.R. (1/s)	Modulus (GPa)	Fail.Mod.(GPa)	Yield (MPa)
JA2	0	100	1.18	-.018	40.3
JA2	0	.01	0.55	-.008	12.8
JA2	60	100	0.28	-.020	5.6
JA2	60	.01	0.08	-.005	1.9
M30	0	100	3.23	1.03	118.9
M30	0	.01	1.68	0.21	51.0
M30	60	100	0.94	0.21	42.0
M30	60	.01	0.18	0.02	14.3

displacement. In a later section, it is shown that the combustion characteristics of M30 specimens 5, 8 and 15 deviate significantly from the combustion characteristics of baseline undamaged propellant.

The compressive modulus and yield stress in these materials increase as temperature decreases and strain rate increases, although temperature dominates the effect over the test condition range. In addition, the absolute value of the failure modulus[3] (negative slope of post-yield stress versus strain curve) increases as temperature decreases (except for JA2) and strain rate increases although, strain rate dominates the effect over the test condition range (Table 3).

4.2 Propellant Combustion Characteristics This section outlines the results of the burn rate analysis obtained as a result of mini closed-bomb pressure chamber tests on damaged and baseline M30 and JA2 propellants. A complete description of the PC-based burn rate analysis program can be found in Oberle and Kooker[9]. Plots of apparent burn rate versus pressure reveal that the combustion response of damaged JA2 is not nearly as variable as the combustion response of damaged M30 over the range of test conditions (Figure 10). The vertical line in Figure 10 depicts the lowest pressure over which the burn rate versus pressure response is linear for both propellants. The apparent burn rates at this pressure are used in a subsequent section to characterize the combustion response of the propellant as a function of strain rate, temperature, and percent axial strain. An empirical relation between apparent burn rate, R, and pressure, P, (Equation 2) is fit to the data (Figure 10), and the coefficients, n versus a, are plotted for the sixteen experiments and four baseline tests (Figure 11). It is interesting to note that n is a power-law in a for damaged and undamaged propellant, where a represents the apparent burn rate at 1 MPa pressure and n is the pressure power-coefficient. The wider range in n versus a values for the fracture-damaged M30 propellant illustrates the greater variability in burn rate response relative to JA2 propellant over the range of test conditions.

5. DISCUSSION

An apparent burn rate response surface, R, is generated to determine the relative linear and nonlinear contributions of the independent variables. In this work, the empirical apparent burn rate response surface, R, is written as a second-order polynomial expansion of the four independent variables, (X_1=propellant, X_2=strain rate, X_3=% strain, and X_4=temperature) as:

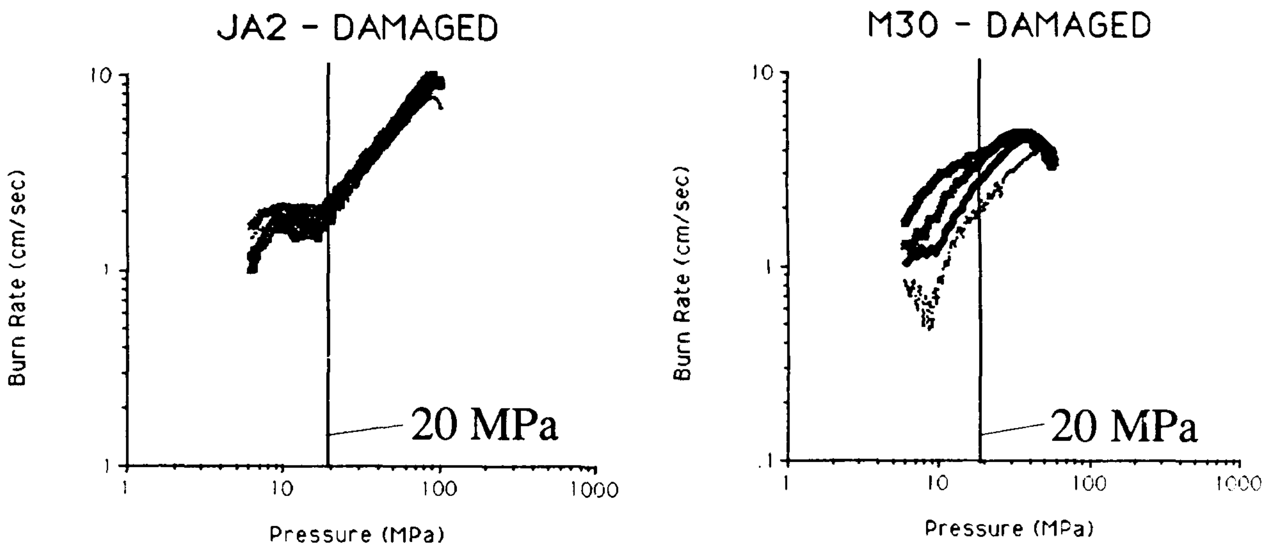

Figure 10. Apparent Burn Rates of Damaged JA2 and M30 Propellants. Coordinate Axes are Log Base 10.

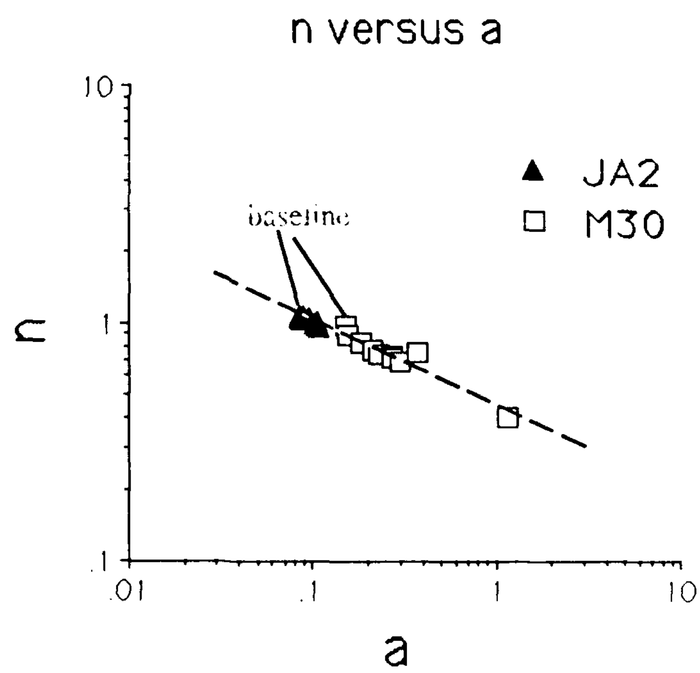

Figure 11. Comparison of Burn Rate Coefficients, n and a, (Equation 2) for Damaged and Undamaged (Baseline) Propellant. The Coefficients are Determined for the Range from 25 % to 75 % Maximum Pressure. Coordinate Axes are Log Base 10.

$$R_{(20\ MPa)} = b_0 + b_1X_1 + b_2X_2 + b_3X_3 + b_4X_4 + b_{12}X_1X_2 + b_{13}X_1X_3 + b_{14}X_1X_4 + b_{23}X_2X_3 + b_{24}X_2X_4 + b_{34}X_3X_4 \qquad (3)$$

or, more generally as:

$$R = b_0 + \sum_{i=1}^{q} b_iX_i + \sum_{i=1}^{q}\sum_{j \geq i}^{q} b_{ij}X_iX_j$$

where, $b_o = \sum_{i=1}^{n} R_i/n$ and q = number of factors, n = total no. of experiments.

The b_i quantify the main effects of the independent controllable variables. The b_{ij} terms describe the pairwise interaction effects of the independent variables. The intercept term, b_o, is simply the arithmetic mean of all the recorded responses. The second-order polynomial model is fit to the data using standard least squares regression techniques. The numerical values of the independent variables, X_i, are standardized (nondimensionalized) to range from +1 for "high" experimental test conditions, and -1 for "low" experimental test conditions. Nondimensionalizing the variables allows one to rank the coefficients (determined by least squares regression analysis) by magnitude to determine the relative contribution of each variable to the measured response. An inspection of the coefficients in the second-order polynomial expansion will permit one to determine the relative contributions of each of the independent variables to the burn rate of M30 and JA2 gun propellants. Thus, a hierarchy is established which ranks the relative importance of the independent variables over the test range.

The apparent burn rate at 20 MPa is used as the combustion response, R. The burn rate at 20 MPa is chosen to characterize the combustion response because the log burn rate versus log pressure response for both propellants is relatively linear at this pressure. A regression analysis[14] is performed and the coefficients and their relative rankings appear in Table 4. The results of the regression analysis indicate that the interaction propellant type*strain is the most significant factor controlling the burn rate at 20 MPa. The second most significant factor is the propellant type. The third, fourth, and fifth most significant factors (at the alpha = .05 confidence level) are the percent axial strain, deformation temperature, and interaction strain*temperature, respectively. The apparent burn rates of these propellants are virtually independent of the deformation strain rate. This result is surprising insofar as in a

Table 4. Coefficients and Rankings for Predicting the Apparent Burn Rate (@ 20 MPa) of M30 and JA2 Propellants (Combined Analysis). The Coefficients Ranked 1,2,3,4, and 5 are Significant at the Alpha = .05 Confidence Level.

Factors	Coefficients	Rank
Propellant	**-.2820**	**2**
Strain Rate	.0030	10
Strain	**.2130**	**3**
Temperature	**-.2130**	**4**
Propellant*S. R.	.0660	7
Propellant*Strain	**-.2900**	**1**
Propellant*Temp.	.1330	6
Strain Rate*Strain	.0150	9
Strain Rate*Temp.	-.0580	8
Strain*Temp.	**-.1720**	**5**
Constant	2.365	
R-square(adj.)	0.822	
RMS Residual	0.250	

Table 5. Coefficients and Rankings for Predicting the Apparent Burn Rate (@ 20 MPa) of M30 and JA2 Propellants (Separate Analysis).

Factors	Coefficients		Ranks	
	M30	JA2	M30	JA2
Strain Rate	-.063	.070	5	4
Strain	**.502**	-.077	**1**	2
Temperature	-.342	**-.083**	2	**1**
Strain Rate*Strain	-.031	.062	6	5
Strain Rate*Temp.	-.108	-.007	4	6
Strain*Temp.	-.272	-.072	3	3
Constant	2.646	2.083		
R-square(adj.)	0.863	0.861		
RMS Residual	0.270	0.066		

previous section it is shown that the mechanical response of these propellants, as characterized by the compressive modulus, yield stress, and failure modulus, is a strong function of the deformation strain rate over the same test condition range. In addition, theoretical and observational studies of a variety of materials indicate that fragmentation size is a strong function of loading rate. Fragment sizes tend to be larger at slow rates of loading and fragment sizes are smaller and more highly comminuted at dynamic rates of loading[8]. It is apparent then, that relative to the other independent variables, the apparent burn rate for these propellants is insensitive to strain rate over the range 10^{-2} to 100 sec^{-1}.

Since propellant type is a discrete independent variable, and a dominant factor controlling the apparent burning rates, an analysis is carried out whereby the regression analysis is performed for each propellant separately. Table 5 illustrates the results of the separate regression analyses and ranks the factors as in the previous example. In this analysis however, significance levels are not established because the estimate of experimental error is associated with only one degree of freedom in the system (8 data points minus 7 coefficients).

The regression analysis reveals that the apparent burn rate of M30 is dominated by the axial strain followed by deformation temperature. In contrast, the apparent burn rate of JA2 is dominated by deformation temperature followed by axial strain level. In addition, the apparent burn rate of JA2 decreases as the strain level increases, yet the apparent burn rate of M30 increases as the strain level increases. This result is attributed to an increase in fracture-induced surface area in M30 relative to purely dimensional changes in JA2. Figure 12 illustrates the actual and predicted burn rates for these propellants at 20 MPa determined using coefficents in Table 5.

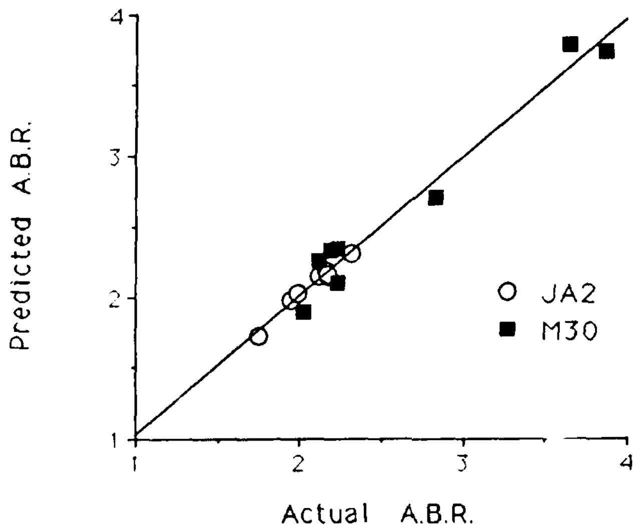

Figure 12. Predicted versus Actual Apparent Burn Rates (A.B.R.) in cm/sec Calculated Using Coefficients in Table 5.

5.1 Surface Area Analysis In order to determine the amount of fracture surface area generated as a result of damage, Equation 1 is first solved for surface area, A. A measure of the amount of fracture induced damage relative to the undamaged baseline propellant is given by the surface area ratio, Sd/Su:

$$Sd(t)/Su(t) = dm_d/dm_u$$

where, dm_d and dm_u are the incremental masses generated per unit time in the damaged and undamaged propellants respectively. It is assumed that the burn rates and densities of the damaged and undamaged propellant are identical. The time dependent surface area ratio is a function of the incremental mass generation rate, which in turn is a function of the incremental pressurization rate of the chamber. This measure is useful since it is independent of specimen geometry and reflects changes in damage-induced surface area relative to the baseline propellant. Surface area ratio plots for all sixteen M30 tests are illustrated in Figure 13. The plots are partitioned on the dominant factor (percent axial strain) controlling the apparent burn rate in M30 propellant. The effect of fracture-induced damage is also illustrated by examining pressurization rate profiles. The maximum pressurization rates for the damaged M30 (4.5 MPa/msec) are about the same as for undamaged baseline specimens, however for damaged specimens the maxima occur at earlier times than the undamaged specimens (except for test #13, Figure 14).

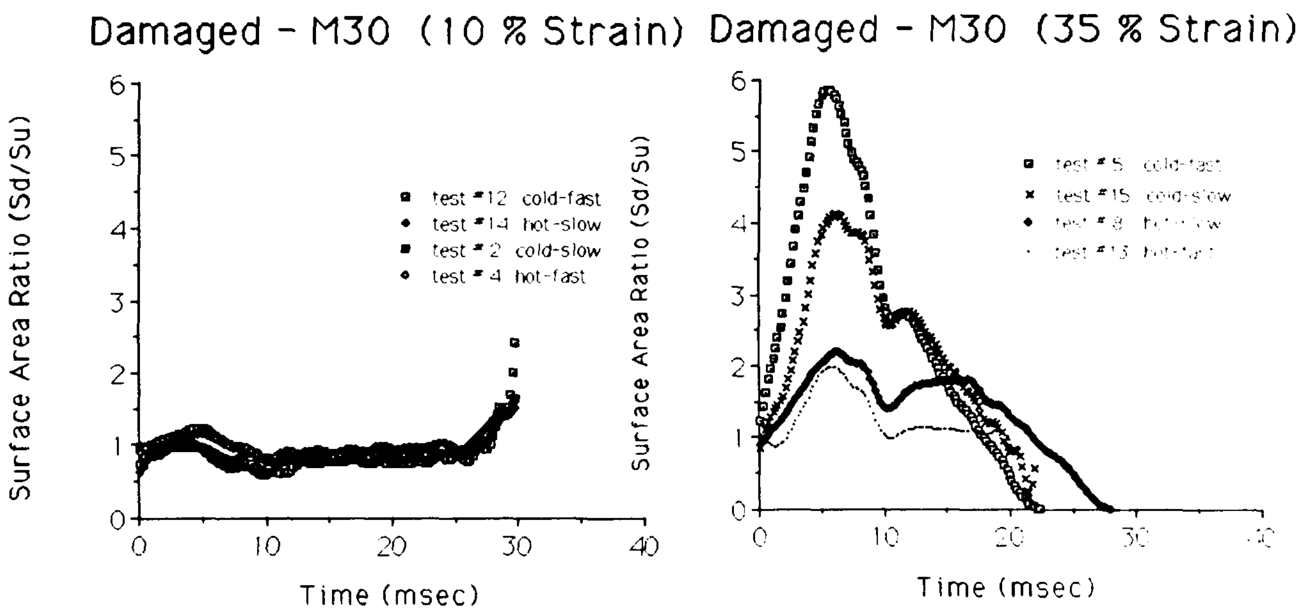

Figure 13. Surface Area Ratio Plots versus Time Showing How Percent Axial Strain Dominates the Apparent Burn Rate of M30 Propellant.

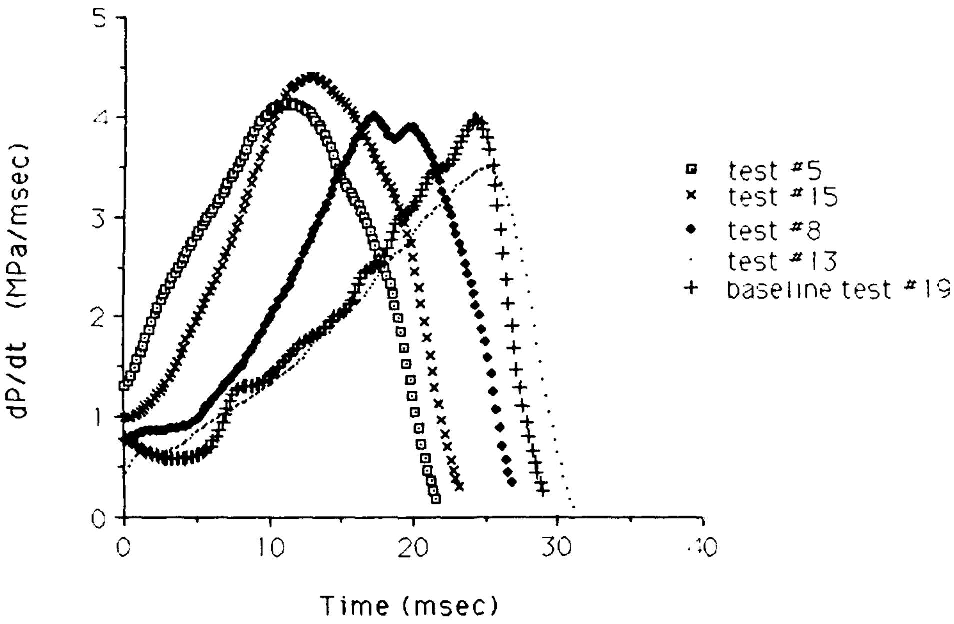

Figure 14. Pressurization Rate versus Time for Damaged/Undamaged M30 Propellant (see also Figure 13 for Surface Area Comparison).

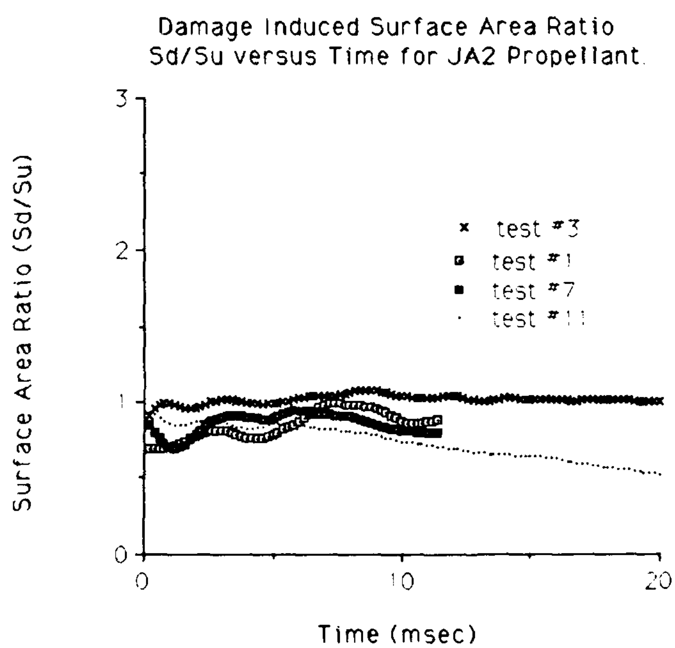

Figure 15. Damage-Induced Surface Area Ratio versus Time for JA2 Propellant.

The surface area ratio plots can either be plotted as a function of mass fraction burnt, time, or P/Pmax. The surface area ratio for JA2 remains near unity over the entire spectrum of test conditions and indicates that over the test range anomalous surface area is not generated in the material relative to the baseline undamaged propellant (Figure 15). JA2 begins to fracture in uniaxial compression as the temperature is decreased below the glass transition temperature (-20 degrees Celsius), or as the specimen aspect ratio, length-to-diameter ratio, increases[6]. In contrast, the surface area ratio for M30, deformed to 35 percent axial strain, reaches six times that of the undamaged baseline propellant. Surface area ratios in tests # 5, 8, 13, and 15 depart significantly from unity and this is not surprising since numerous visible cracks are present in these specimens (Figure 9).

6. CONCLUSIONS

1) The use of a well designed testing approach maximizes the information obtainable concerning the sensitivity of combustion characteristics of M30 and JA2 gun propellants to the effects of strain rate, temperature, and percent axial strain, while simultaneously minimizing the number of tests involved.

2) Experimental design methods can provide an empirically derived model for quantifying factor effects within the test range and provide a means for establishing a hierarchy of factor effect importance.

3) The apparent burn rates of damaged JA2 propellant are relatively unaffected by the induced deformation. Results of the statistical test design indicate that the apparent burn rate of JA2 at 20 MPa is primarily dependent on the deformation temperature.

4) The apparent burn rates of damaged M30 propellant vary considerably and the degree of damage-induced surface area approaches six times that of the undeformed baseline M30 specimens. Results of the statistical test design indicate that the apparent burn rate of M30 at 20 MPa is dependent primarily on percent axial specimen strain.

5) The apparent burn rates for these propellants are relatively insensitive to the deformation strain rate over the range 10^{-2} to 100 sec^{-1}, yet a number of observational and theoretical studies show that fragmentation size is a function of loading rate. The observation that the apparent burn rate is insensitive to deformation strain rate is also surprising given that the mechanical properties of these materials are strongly strain rate dependent.

6) The insensitivity of the apparent burn rate to strain rate may in part be due to the limited strain rate range investigated 10^{-2} to 100 sec^{-1} and in part due to the dominance of the other factors, temperature and percent axial specimen strain. Second-order strain rate effects may be realizable at large specimen strains.

7) If deformation strain rate does not significantly affect the apparent burn rates of these propellants (relative to percent axial strain and temperature) then it may not be necessary to determine high loading rate mechanical properties for these materials. This information is useful for interior ballistic models which at present only track intergranular stress as a criterion for grain failure.

8) A unique relationship between propellant mechanical properties and propellant combustion characteristics does not exist for JA2 propellant, since the mechanical properties of JA2 gun propellant change dramatically with temperature and strain rate, while the combustion characteristics remain relatively uniform. Whether these findings hold for a wider class of propellants still needs to be determined.

7. FUTURE WORK

Future work should examine whether the observation that the apparent burn rate is relatively insensitive to deformation strain rate can be generalized to include a wider class of energetic materials. Uniaxial compression tests on energetic materials whose macrocscopic deformation mechanisms are dominated by fracturing will be performed using statistical design, but under an expanded strain rate window, the upper limit of which will include dynamic strain rates (10^3 sec^{-1}). If it can be shown that the combustion of these materials is relatively insensitive to deformation strain rate, then this will greatly simplify interior ballistic numerical model development, which presently tracks changes in bed porosity (combining both grain deformations and rigid body motions) and intergranular stress in a rudimentary model of grain fracture.

7. REFERENCES

1. R.A. Fifer and J.E. Cole, "Transitions from Laminar Burning for Porous Crystalline Explosives.", in: Proceedings of the 7th Symposium (International) on Detonation, Annapolis, MD, pp. 164-174, June 16-19, 1981.

2. R.J. Lieb, D. Devynck, and J.J. Rocchio, "The Evaluation of High Rate Fracture Damage of Gun Propellant." 1983 JANNAF Structures and Mechanics Subcommittee Meeting, CPIA Pub. # 388, pp. 177-185, November, 1983.

3. R.J. Lieb, "Impact-Generated Surface Area in Gun Propellants." BRL-TR-2946, U.S. Army Ballistic Research Laboratory, Aberdeen Proving Ground, MD, November, 1988.

4. P.S. Gough, "The NOVA Code: A User's Manual.", Indian Head Contract Report IHCR80-8, Naval Ordnance Station, Indian Head, MD, 1980.

5. G.A. Gazonas, "The Mechanical Response of M30, XM39, and JA2 Propellants at Strain Rates from 10^{-2} to 250 sec^{-1}" BRL-TR-3181, U.S. Army Ballistic Research Laboratory, Aberdeen Proving Ground, MD, January, 1991.

6. G.A. Gazonas, D.A. Hopkins, and J.C. Ford, "Experimental Determination of Critical Physical Parameters Affecting JA2 Propellant Grain Response, Phase I: Screening Design." BRL-TR-3237, U.S. Army Ballistic Research Laboratory, Aberdeen Proving Ground, MD, May 1991.

7. S.R. Swanson, "A Calculation Model for Fragmentation in Viscoelastic Materials." 16th JANNAF Combustion Meeting, CPIA Pub. # 308, Vol. I, pp. 167-176, December, 1979.

8. D.E. Grady and M.E. Kipp, "Dynamic Rock Fragmentation." Fracture Mechanics of Rock, Academic Press Inc., London, Sandia National Laboratories, pp. 429-445, Albuquerque, NM, 1987.

9. W.F. Oberle III, and D.E. Kooker, "BRLCB: A Closed Chamber Data Analysis Program with Provisions for Deterred and Layered Propellants." BRL-TR-3227, U.S. Army Ballistic Research Laboratory, Aberdeen Proving Ground, MD, April, 1991.

10. W.F Oberle III, A.A. Juhasz, and T. Griffie, "A Simplified Computer Code for Reduction to Burning Rates of Closed Bomb Pressure-Time Data (MINICB)." BRL-TR-2841, U.S. Army Ballistic Research Laboratory, Aberdeen Proving Ground, MD, August, 1981.

11. M.S. Miller, "Flamespreading Measurements and Mechanisms in Perforated LOVA Gun Propellants." 23rd JANNAF Combustion Meeting Proceedings, CPIA Pub. # 457, Vol. II, pp. 329-335, October, 1986.

12. G.E.P. Box, W.G. Hunter, and J.S. Hunter, Statistics for Experimenters. New York, N.Y., John Wiley and Sons Publishing Co., 1978.

13. W. Mendenhall, Introduction to Probability and Statistics, 4th Edition, Duxbury Press, 1975.

14. StatView™ II, Version 1.03, Abacus Concepts, Inc., Berkeley, CA, 1987.

INTENTIONALLY LEFT BLANK.

No. of Copies	Organization
2	Administrator Defense Technical Info Center ATTN: DTIC-DDA Cameron Station Alexandria, VA 22304-6145
1	Commander U.S. Army Materiel Command ATTN: AMCDRA-ST 5001 Eisenhower Avenue Alexandria, VA 22333-0001
1	Commander U.S. Army Laboratory Command ATTN: AMSLC-DL 2800 Powder Mill Road Adelphi, MD 20783-1145
2	Commander U.S. Army Armament Research, Development, and Engineering Center ATTN: SMCAR-IMI-I Picatinny Arsenal, NJ 07806-5000
2	Commander U.S. Army Armament Research, Development, and Engineering Center ATTN: SMCAR-TDC Picatinny Arsenal, NJ 07806-5000
1	Director Benet Weapons Laboratory U.S. Army Armament Research, Development, and Engineering Center ATTN: SMCAR-CCB-TL Watervliet, NY 12189-4050
(Unclass. only) 1	Commander U.S. Army Armament, Munitions and Chemical Command ATTN: AMSMC-IMF-L Rock Island, IL 61299-5000
1	Director U.S. Army Aviation Research and Technology Activity ATTN: SAVRT-R (Library) M/S 219-3 Ames Research Center Moffett Field, CA 94035-1000
1	Commander U.S. Army Missile Command ATTN: AMSMI-RD-CS-R (DOC) Redstone Arsenal, AL 35898-5010
1	Commander U.S. Army Tank-Automotive Command ATTN: ASQNC-TAC-DIT (Technical Information Center) Warren, MI 48397-5000
1	Director U.S. Army TRADOC Analysis Command ATTN: ATRC-WSR White Sands Missile Range, NM 88002-5502
1	Commandant U.S. Army Field Artillery School ATTN: ATSF-CSI Ft. Sill, OK 73503-5000
(Class. only) 1	Commandant U.S. Army Infantry School ATTN: ATSH-CD (Security Mgr.) Fort Benning, GA 31905-5660
(Unclass. only) 1	Commandant U.S. Army Infantry School ATTN: ATSH-CD-CSO-OR Fort Benning, GA 31905-5660
1	Air Force Armament Laboratory ATTN: WL/MNOI Eglin AFB, FL 32542-5000
	<u>Aberdeen Proving Ground</u>
2	Dir, USAMSAA ATTN: AMXSY-D AMXSY-MP, H. Cohen
1	Cdr, USATECOM ATTN: AMSTE-TC
3	Cdr, CRDEC, AMCCOM ATTN: SMCCR-RSP-A SMCCR-MU SMCCR-MSI
1	Dir, VLAMO ATTN: AMSLC-VL-D
10	Dir, BRL ATTN: SLCBR-DD-T

No. of Copies	Organization
1	HQDA (SARDA) WASH DC 20310-2500
1	Commander U.S. Army TSARCOM 4300 Goodfellow Boulevard St. Louis, MO 63120-1702
1	Commander U.S. Army Missile and Space Intelligence Center ATTN: AIAMS-YDL Redstone Arsenal, AL 35898-5500
1	Commander U.S. Army Tank-Automotive Command ATTN: AMSTA-CG Warren, MI 48090
1	Commander U.S. Army TRAC-Ft. Lee Defense Logistics Studies Fort Lee, VA 23801-6140
1	Commander USA Concepts Analysis Agency ATTN: D. Hardison 8120 Woodmont Avenue Bethesda, MD 20014-2797
10	Central Intelligence Agency Office of Central Reference Dissemination Branch Room GE-47 HQS Washington, DC 20505
1	U.S. Army Ballistic Missile Defense Systems Command Advanced Technology Center P.O. Box 1500 Huntsville, AL 35807-3801

No. of Copies	Organization
1	Chairman DoD Explosives Safety Board Room 856-C Hoffman Bldg. 1 2461 Eisenhower Avenue Alexandria, VA 22331-0600
1	Commander U.S. Army Materiel Command ATTN: AMCDE-DW 5001 Eisenhower Avenue Alexandria, VA 22333-5001
1	Commander U.S. Army Materiel Command ATTN: AMCICP-AD, Michael F. Fisette 5001 Eisenhower Avenue Alexandria, VA 22333-5001
1	Department of the Army Office of the Product Manager 155mm Howitzer, M109A6, Paladin ATTN: SFAE-AR-HIP, IP, Mr. R. De Kleine Picatinny Arsenal, NJ 07806-5000
1	Project Manager Production Base Modernization Agency ATTN: AMSMC-PBM-E, L. Laibson Picatinny Arsenal, NJ 07806-5000
3	PEO-Armaments Project Manager Tank Main Armament Systems ATTN: AMCPM-TMA, K. Russell AMCPM-TMA-105 AMCPM-TMA-120 Picatinny Arsenal, NJ 07806-5000
3	Commander U.S. Army Armament Research, Development, and Engineering Center ATTN: SMCAR-HFM, E. Barrieres R. Davitt SMCAR-CCH-V, C. Mandala Picatinny Arsenal, NJ 07806-5000

No. of Copies	Organization
8	Commander U.S. Army Armament Research, Development, and Engineering Center ATTN: SMCAR-AEE-B, A. Beardell B. Brodman D. Downs S. Einstein S. Westley S. Bernstein C. Roller J. Rutkowski Picatinny Arsenal, NJ 07806-5000
1	Commander U.S. Army Armament Research, Development, and Engineering Center ATTN: SMCAR-AES, S. Kaplowitz, Bldg. 321 Picatinny Arsenal, NJ 07806-5000
1	Commander U.S. Army Armament Research, Development, and Engineering Center ATTN: SMCAR-FSA-T, M. Salsbury Picatinny Arsenal, NJ 07806-5000
1	Commander, USACECOM R&D Technical Library ATTN: ASQNC-ELC-IS-L-R, Myer Center Fort Monmouth, NJ 07703-5000
1	Commander U.S. Army Harry Diamond Laboratories ATTN: SLCHD-TA-L 2800 Powder Mill Rd Adelphi, MD 20783-1145
1	Commandant U.S. Army Aviation School ATTN: Aviation Agency Fort Rucker, AL 36360
2	Program Manager U.S. Army Tank-Automotive Command ATTN: SFAE-ASM-SS-T, T. Dean Warren, MI 48092-2498

No. of Copies	Organization
1	Project Manager U.S. Army Tank-Automotive Command Fighting Vehicle Systems ATTN: AMCPM-BFVS Warren, MI 48092-2498
1	President U.S. Army Armor and Engineer Board ATTN: ATZK-AD-S Fort Knox, KY 40121-5200
1	Project Manager U.S. Army Tank-Automotive Command ATTN: AMCPM-ABMS Warren, MI 48092-2498
1	Director HQ, TRAC RPD ATTN: ATRC-MA, MAJ Williams Fort Monroe, VA 23651-5143
2	Director U.S. Army Materials Technology Laboratory ATTN: SLCMT-ATL Watertown, MA 02172-0001
1	Commander U.S. Army Research Office ATTN: Technical Library P. O. Box 12211 Research Triangle Park, NC 27709-2211
1	Commander U.S. Army Belvoir Research and Development Center ATTN: STRBE-WC Fort Belvoir, VA 22060-5006
1	Director U.S. Army TRAC-Ft Lee ATTN: ATRC-L, Mr. Cameron Fort Lee, VA 23801-6140
1	President U.S. Army Artillery Board Ft. Sill, OK 73503-5000

No. of Copies	Organization
1	Commandant U.S. Army Special Warfare School ATTN: Rev and Tng Lit Div Fort Bragg, NC 28307
3	Commander Radford Army Ammunition Plant ATTN: SMCAR-QA/HI LIB Radford, VA 24141-0298
1	Commander U.S. Army Foreign Science and Technology Center ATTN: AMXST-MC-3 220 Seventh Street, NE Charlottesville, VA 22901-5396
2	Commander Naval Sea Systems Command ATTN: SEA 62R SEA 64 Washington, DC 20362-5101
1	Commander Naval Air Systems Command ATTN: AIR-954-Technical Library Washington, DC 20360
1	Assistant Secretary of the Navy (R, E, and S) ATTN: R. Reichenbach Room 5E787 Pentagon Bldg Washington, DC 20375
1	Naval Research Laboratory Technical Library Washington, DC 20375
1	Commandant U.S. Army Command and General Staff College Fort Leavenworth, KS 66027
2	Commandant U.S. Army Field Artillery Center and School ATTN: ATSF-CO-MW, B. Willis Ft. Sill, OK 73503-5600

No. of Copies	Organization
1	Office of Naval Research ATTN: Code 473, R. S. Miller 800 N. Quincy Street Arlington, VA 22217-9999
3	Commandant U.S. Army Armor School ATTN: ATZK-CD-MS, M. Falkovitch Armor Agency Fort Knox, KY 40121-5215
2	Commander U.S. Naval Surface Warfare Center ATTN: J. P. Consaga C. Gotzmer Indian Head, MD 20640-5000
4	Commander Naval Surface Warfare Center ATTN: Code 240, S. Jacobs Code 730 Code R-13, K. Kim Code R-10, R. Bernecker Silver Spring, MD 20903-5000
2	Commanding Officer Naval Underwater Systems Center ATTN: Code 5B331, R. S. Lazar Technical Library Newport, RI 02840
5	Commander Naval Surface Warfare Center ATTN: Code G33, J. L. East W. Burrell J. Johndrow Code G23, D. McClure Code DX-21, Technical Library Dahlgren, VA 22448-5000
3	Commander Naval Weapons Center ATTN: Code 388, C. F. Price Code 3895, T. Parr Information Science Division China Lake, CA 93555-6001

No. of Copies	Organization
1	AL/TSTL (Technical Library) ATTN: J. Lamb Edwards AFB, CA 93523-5000
1	AFATL/DLYV Eglin AFB, FL 32542-5000
1	AFATL/DLXP Eglin AFB, FL 32542-5000
1	AFATL/DLJE Eglin AFB, FL 32542-5000
1	NASA/Lyndon B. Johnson Space Center ATTN: NHS-22, Library Section Houston, TX 77054
1	AFELM, The Rand Corporation ATTN: Library D 1700 Main Street Santa Monica, CA 90401-3297
1	Hercules Incorporated ATTN: R. V. Cartwright Howard Boulevard Kenvil, NJ 07847
1	Scientific Research Assoc., Inc. ATTN: H. McDonald P.O. Box 498 Glastonbury, CT 06033-0498
1	United Technologies Corporation Chemical Systems Division ATTN: Tech Library P.O. Box 49028 San Jose, CA 95161-9028
1	AAI Corporation ATTN: J. Frankle P. O. Box 126 Hunt Valley, MD 21030-0126
1	Aerojet General Corporation ATTN: D. Thatcher P.O. Box 296 Azusa, CA 91702

No. of Copies	Organization
1	Aerojet Solid Propulsion Company ATTN: P. Micheli Sarcramento, CA 96813
1	Atlantic Research Corporation ATTN: M. King 5390 Cherokee Avenue Alexandria, VA 22312-2302
3	AL/LSCF ATTN: J. Levine L. Quinn T. Edwards Edwards AFB, CA 93523-5000
1	AVCO Everett Research Laboratory ATTN: D. Stickler 2385 Revere Beach Parkway Everett, MA 02149-5936
2	Calspan Corporation ATTN: C. Murphy P. O. Box 400 Buffalo, NY 14225-0400
1	IITRI ATTN: M. J. Klein 10 W. 35th Street Chicago, IL 60616-3799
1	Hercules, Inc. Allegheny Ballistics Laboratory ATTN: William B. Walkup P. O. Box 210 Rocket Center, WV 26726
1	Hercules, Inc. Radford Army Ammunition Plant ATTN: J. Pierce Radford, VA 24141-0299
3	Lawrence Livermore National Laboratory ATTN: L-355, A. Buckingham M. Finger L-324, M. Constantino P. O. Box 808 Livermore, CA 94550-0622

No. of Copies	Organization
1	Olin Corporation Badger Army Ammunition Plant ATTN: F. E. Wolf Baraboo, WI 53913
1	Olin Ordnance ATTN: V. McDonald, Library P. O. Box 222 St. Marks, FL 32355-0222
1	Paul Gough Associates, Inc. ATTN: Dr. Paul S. Gough 1048 South Street Portsmouth, NH 03801
1	Physics International Company ATTN: Library, H. Wayne Wampler 2700 Merced Street San Leandro, CA 94577-5602
1	Princeton Combustion Research Laboratory, Inc. ATTN: M. Summerfield 475 U.S. Highway One Monmouth Junction, NJ 08852-9650
2	Rockwell International Rocketdyne Division ATTN: BA08, J. E. Flanagan J. Gray 6633 Canoga Avenue Canoga Park, CA 91303-2703
1	Thiokol Corporation Huntsville Division ATTN: Technical Library Huntsville, AL 35807
1	Sverdrup Technology ATTN: Dr. John Deur 2001 Aerospace Parkway Brook Park, OH 44142

No. of Copies	Organization
2	Thiokol Corporation Elkton Division ATTN: R. Biddle Technical Library P. O. Box 241 Elkton, MD 21921-0241
1	Veritay Technology, Inc. ATTN: E. Fisher 4845 Millersport Highway East Amherst, NY 14501-0305
1	Universal Propulsion Company ATTN: H. J. McSpadden Black Canyon Stage 1 Box 1140 Phoenix, AZ 84029
1	Battelle ATTN: TACTEC Library, J. N. Huggins 505 King Ave. Columbus, OH 43201-2693
1	Brigham Young University Department of Chemical Engineering ATTN: M. Beckstead Provo, UT 84601
1	Vanderbilt University Mechanical Engineering ATTN: A. M. Mellor Box 6019, Station B Nashville, TN 37235
1	California Institute of Technology 204 Karman Laboratory Main Stop 301-46 ATTN: F.E.C. Culick 1201 E. California Street Pasadena, CA 91109
1	California Institute of Technology Jet Propulsion Laboratory ATTN: L. D. Strand, MS 512/102 4800 Oak Grove Drive Pasadena, CA 91109-8099

No. of Copies	Organization
1	University of Illinois Department of Mechanical/Industrial Engineering ATTN: H. Krier 144 MEB; 1206 N. Green Street Urbana, IL 61801-2978
1	University of Massachusetts Department of Mechanical Engineering ATTN: K. Jakus Amherst, MA 01002-0014
1	University of Minnesota Department of Mechanical Engineering ATTN: E. Fletcher Minneapolis, MN 55414-3368
3	Georgia Institute of Technology School of Aerospace Engineering ATTN: B.T. Zinn E. Price W.C. Strahle Atlanta, GA 30332
1	Institute of Gas Technology ATTN: D. Gidaspow 3424 S. State Street Chicago, IL 60616-3896
1	Johns Hopkins University Applied Physics Laboratory Chemical Propulsion Information Agency ATTN: T. Christian Johns Hopkins Road Laurel, MD 20707-0690
1	Massachusetts Institute of Technology Department of Mechanical Engineering ATTN: T. Toong 77 Massachusetts Avenue Cambridge, MA 02139-4307
1	Pennsylvania State University Applied Research Laboratory ATTN: G.M. Faeth University Park, PA 16802-7501
1	Pennsylvania State University Department of Mechanical Engineering ATTN: K. Kuo University Park, PA 16802-7501
1	Purdue University School of Mechanical Engineering ATTN: J. R. Osborn TSPC Chaffee Hall West Lafayette, IN 47907-1199
1	SRI International Propulsion Sciences Division ATTN: Technical Library 333 Ravenwood Avenue Menlo Park, CA 94025-3493
1	Rensselaer Polytechnic Institute Department of Mathematics Troy, NY 12181
1	Stevens Institute of Technology Davidson Laboratory ATTN: R. McAlevy, III Castle Point Station Hoboken, NJ 07030-5907
1	Rutgers University Department of Mechanical and Aerospace Engineering ATTN: S. Temkin University Heights Campus New Brunswick, NJ 08903
1	University of Southern California Mechanical Engineering Department ATTN: 0HE200, M. Gerstein Los Angeles, CA 90089-5199
2	University of Utah Department of Chemical Engineering ATTN: A. Baer G. Flandro Salt Lake City, UT 84112-1194
1	Washington State University Department of Mechanical Engineering ATTN: C. T. Crowe Pullman, WA 99163-5201

No. of Copies	Organization
1	Alliant Techsystems, Inc. ATTN: R. E. Tompkins MN38-3300 10400 Yellow Circle Drive Minnetonka, MN 55343
1	Science Applications, Inc. ATTN: R. B. Edelman 23146 Cumorah Crest Drive Woodland Hills, CA 91364-3710
	Aberdeen Proving Ground
	Dir, USAMSAA ATTN: AMXSY-GI, CPT Klimack

USER EVALUATION SHEET/CHANGE OF ADDRESS

This laboratory undertakes a continuing effort to improve the quality of the reports it publishes. Your comments/answers below will aid us in our efforts.

1. Does this report satisfy a need? (Comment on purpose, related project, or other area of interest for which the report will be used.) ______________________________

2. How, specifically, is the report being used? (Information source, design data, procedure, source of ideas, etc.) ______________________________

3. Has the information in this report led to any quantitative savings as far as man-hours or dollars saved, operating costs avoided, or efficiencies achieved, etc? If so, please elaborate. ______________________________

4. General Comments. What do you think should be changed to improve future reports? (Indicate changes to organization, technical content, format, etc.) ______________________________

BRL Report Number BRL-TR-3251 Division Symbol ____________

Check here if desire to be removed from distribution list. ____

Check here for address change. ____

Current address: Organization ______________________
Address ______________________

DEPARTMENT OF THE ARMY

Director
U.S. Army Ballistic Research Laboratory
ATTN: SLCBR-DD-T
Aberdeen Proving Ground, MD 21005-5066

OFFICIAL BUSINESS

NO POSTAGE NECESSARY IF MAILED IN THE UNITED STATES

BUSINESS REPLY MAIL

FIRST CLASS PERMIT No 0001, APG, MD

Postage will be paid by addressee

Director
U.S. Army Ballistic Research Laboratory
ATTN: SLCBR-DD-T
Aberdeen Proving Ground, MD 21005-5066